

IN-MEDIUM ω -MESON BROADENING AND S-WAVE
PION ANNIHILATION INTO e^+e^- PAIRS

Gyuri Wolf

*GSI, Planckstrasse 1
D-64291 Darmstadt, Germany
CRIP, H-1525 Budapest, Hungary*

Bengt Friman

*GSI, Planckstrasse 1
D-64291 Darmstadt, Germany
Institut für Kernphysik, TH Darmstadt
D-64289 Darmstadt, Germany*

and

Madeleine Soyeur

*Commissariat à l'Energie Atomique
Laboratoire National Saturne, CE de Saclay
F-91191 Gif-sur-Yvette Cedex, France*

Abstract

An ω -meson in motion with respect to a nuclear medium can couple to a σ -meson through a particle-hole excitation. This coupling is large. We investigate its consequences for the width of ω -mesons in matter and for the s-wave annihilation of pions into lepton pairs in relativistic heavy ion collisions. We find that the two pion decay of ω -mesons, resulting from the $\omega - \sigma$ transition and subsequent 2π decay of the σ -meson, leads to a substantial broadening of ω -mesons in matter and possibly to an observable effect in experiments measuring the e^+e^- decay of vector mesons produced in nuclei and in relativistic heavy-ion collisions. The inverse process in relativistic heavy ion collisions, the s-wave annihilation of pions into ω -mesons decaying into e^+e^- pairs, contributes rather little to the total e^+e^- pair production.

1. Introduction

A meson which interacts with a nuclear medium and propagates with respect to this medium with a 3-momentum $\vec{q} \neq 0$ does not have well-defined quantum numbers as in free space. Both continuous space-time symmetries (such as Lorentz invariance) and discrete symmetries (parity, charge conjugation, G-parity) can be broken. For example, the motion of the meson introduces a spatial direction which breaks rotational invariance and allows for the mixing of meson states of different total angular momenta. To lowest order, this mixing is generated by the coupling of the mesons to particle-hole excitations. We restrict ourselves to symmetric nuclear matter, a situation in which isospin is conserved.

Of particular interest is the mixing of vector and scalar mesons in nuclear matter. In the isovector channel, the ρ -exchange is a major part of the short-range particle-hole interaction which inhibits pion condensation [1]. In the isoscalar channel, the coupling of the σ and ω fields through particle-hole excitations is extremely large and is therefore expected to strongly affect the propagation of ω -mesons in nuclear matter [2].

In view of the role that vector mesons play both in hadronic physics and in nuclear dynamics, the propagation of ρ - and ω -mesons in matter is at present the subject of many theoretical investigations. These studies have been largely motivated by the suggestion that in-medium vector meson masses could be order parameters for chiral symmetry restoration at large baryon density [3]. In this case, the masses of the ρ - and ω -mesons would decrease with increasing density as a consequence of their close relation to the quark condensate. To test this idea, measurements of the e^+e^- spectrum of vector mesons produced in nuclei and in heavy ion collisions are planned at TJNAF [4] and GSI [5]. The kinematics is chosen so that at least ρ -mesons decay inside the nuclear medium. We recall that the $\rho(770)$ and $\omega(782)$ have similar masses but very different widths, $\Gamma_\rho = (151.2 \pm 1.2)$ MeV and $\Gamma_\omega = (8.43 \pm 0.10)$ MeV, corresponding to propagation lengths of $c\tau_\rho = 1.3$ fm and $c\tau_\omega = 23.4$ fm in free space [6]. The e^+e^- spectrum will reflect the spectral function of vector meson-like excitations in matter. At sufficiently low density and temperature, it is expected that these excitations will behave as quasi-particles which can be characterized by a mass and a width.

The in-medium width of ρ - and ω -mesons plays a major role in the observability of their in-medium mass. The in-medium widths of vector mesons determine their mean free path in matter and the probability that they decay inside the nuclear target (or in the interaction region for heavy ion collisions) after they are produced. In this respect, the medium broadening of the ω -meson is particularly important because it could make its lifetime comparable to the size of the nuclear system in which it is produced.

The dynamical broadening of ω -mesons in matter can come from various processes [7]. Collisional broadening is expected from the $\omega N \rightarrow \pi N$ reaction which has a large cross section [8] and can cause a significant absorption of ω -mesons into the pion channel. The $\omega N \rightarrow \rho N$ reaction can also play a role and lead to the absorption of ω -mesons into the p-wave two-pion channel. In this paper, we work out the additional width of ω -mesons in matter arising from the large $\omega\sigma$ mixing in matter. The σ meson is an effective degree of freedom

which parametrizes the propagation of two pions in s-wave. The coupling of the ω to the σ in matter opens therefore a new two pion decay channel for the ω -meson. We show that the associated broadening of the ω -meson is large and increases with baryon density as well as with the momentum of the ω -meson. Conversely, the in-medium coupling of the σ to the ω makes it possible for two pions in s-wave to annihilate into a lepton pair through an intermediate ω -meson. We discuss the consequences of this new annihilation channel for the production of e^+e^- pairs in relativistic heavy ion collisions.

In Section 2, we compute the $\omega\sigma$ polarization at finite density and temperature in the one-loop approximation. The $\sigma\pi\pi$ coupling constant and the σ mass are fitted to the $\pi\pi$ s-wave scattering phase shifts in Section 3. Our numerical results for the in-medium ω broadening and the s-wave pion annihilation into e^+e^- pairs in relativistic heavy ion collisions are discussed in Section 4 and we conclude with a brief discussion in Section 5.

2. Calculation of the $\omega\sigma$ polarization

The polarization operator describing the mixing of σ - and ω -mesons to lowest order in matter is shown in Fig. 1. At sufficiently low temperatures, it is dominated by intermediate nucleon-hole states. The two processes discussed in this paper, the broadening of the ω -meson and the s-wave annihilation of pions at finite baryon density and temperature, are directly linked to the polarization operator, as indicated by the diagrams of Fig. 2.

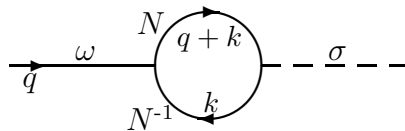


Fig. 1. The $\omega\sigma$ polarisation in nuclear matter.

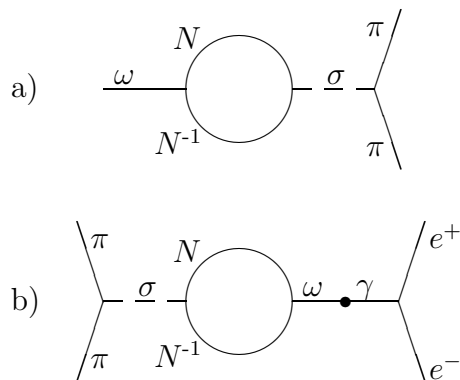


Fig. 2. In-medium $\omega\sigma$ mixing contributions to the ω -meson width (a) and to the s-wave $\pi^+\pi^- \rightarrow e^+e^-$ process (b).

We calculate the polarization operator of Fig. 1 in the relativistic mean-field approximation. Nuclear matter is treated as a system of noninteracting fermions at finite density and temperature. We use free space meson fields. The σ - and ω -meson fields couple to the scalar baryon density and to the conserved baryon current respectively,

$$\mathcal{L}_{\sigma NN} = g_\sigma \bar{\Psi} \sigma \Psi \quad (1)$$

and

$$\mathcal{L}_{\omega NN} = -g_\omega \bar{\Psi} \gamma_\mu \omega^\mu \Psi. \quad (2)$$

The $\omega\sigma$ polarization at finite density and temperature is evaluated in the rest frame of the nuclear matter. We generalize methods used previously [2,9,10] in calculations restricted to matter at zero temperature. The polarization tensor for the process shown in Fig. 1 is given by the expression,

$$-i\Pi^\mu = -2 g_\sigma g_\omega \int \frac{d^4k}{(2\pi)^4} Tr[\gamma^\mu iG(k+q) iG(k)], \quad (3)$$

where $iG(k)$ is the full propagator of a nucleon in nuclear matter at finite temperature. The minus sign arises from the fermion loop and the factor of 2 is the isospin degeneracy factor for symmetric nuclear matter. The full nucleon propagator can be written as the sum of two terms,

$$iG(k) = iG_0(k) + iG_M(k), \quad (4)$$

the free propagator $iG_0(k)$ and a medium term $iG_M(k)$. At zero temperature, the latter allows for the propagation of holes in the Fermi sea and restricts particle propagation to states above the Fermi surface.

In the mean-field approximation, and neglecting the contribution of thermally excited antibaryons, the nucleon propagator reads

$$iG(k) = i(k + M_N^*) \left\{ \frac{1}{k^2 - M_N^{*2} + i\epsilon} + \frac{i\pi}{E^*(k)} \delta[k^0 - E^*(k)] n_T(k) \right\}, \quad (5)$$

where we have introduced the nucleon effective mass M_N^* , the effective kinetic energy $E^*(k) = (\vec{k}^2 + M_N^{*2})^{1/2}$ and the nucleon thermal distribution function $n_T(k)$

$$n_T(k) = \frac{1}{1 + \exp\{[E^*(k) - \mu]/k_B T\}}. \quad (6)$$

In Eq. (6), μ is the chemical potential and k_B the Boltzmann constant. At zero temperature, the thermal distribution function $n_T(k)$ is replaced by the step function $\theta(k_F - |\vec{k}|)$.

Evaluating the trace, we have

$$\begin{aligned}
-i\Pi^\mu = 8 M_N^* g_\sigma g_\omega \int \frac{d^4 k}{(2\pi)^4} (2k+q)^\mu & \left\{ \frac{1}{k^2 - M_N^{*2} + i\epsilon} + \frac{i\pi}{E^*(k)} \delta[k^0 - E^*(k)] n_T(k) \right\} \\
& \left\{ \frac{1}{(k+q)^2 - M_N^{*2} + i\epsilon} + \frac{i\pi}{E^*(k+q)} \delta[k^0 + q^0 - E^*(k+q)] n_T(k+q) \right\}. \quad (7)
\end{aligned}$$

We need Π^μ only for time-like values of q^2 . The product of the propagators gives four terms. The first one is the vacuum polarization which is zero. The product of the matter terms vanishes for time-like q^2 as the constraints from the δ -functions, $\delta[k^0 - E^*(k)]$ and $\delta[k^0 + q^0 - E^*(k+q)]$, are in this case incompatible. We are left with the two terms linear in n_T , which are free of divergences.

The polarization Π^μ satisfies

$$q_\mu \Pi^\mu = 0, \quad (8)$$

as the ω -field is coupled to a conserved current. We choose a coordinate system such that \vec{q} is along the z axis, i.e. $q_\mu = (q_0, 0, 0, q_z)$. The x and y components of the polarization vanish in this frame as there is no motion along the x and y axes. In this case, Eq. (8) implies

$$q_0 \Pi_0 = q_z \Pi_z, \quad (9)$$

i.e. there is only one independent component in the polarization tensor. We calculate Π^0 . After integration over k^0 and a change of variable $\vec{k} \rightarrow \vec{k} + \vec{q}$ in the second term, we obtain

$$\begin{aligned}
\Pi^0 = 8 M_N^* g_\sigma g_\omega \int \frac{d^3 \vec{k}}{(2\pi)^3} & \left\{ \frac{1}{2E^*(k)} \frac{2E^*(k) + q^0}{E^*(k+q)^2 - [E^*(k) + q^0]^2 - i\epsilon} n_T(k) \right. \\
& \left. + \frac{1}{2E^*(k)} \frac{2E^*(k) - q^0}{E^*(k-q)^2 - [E^*(k) - q^0]^2 - i\epsilon} n_T(k) \right\} \quad (10)
\end{aligned}$$

$$\equiv \Pi_1^0 + \Pi_2^0. \quad (11)$$

Clearly, Π^0 is invariant separately under $q_0 \rightarrow -q_0$ and $\vec{q} \rightarrow -\vec{q}$, while Π_z is odd under those transformations. It is then sufficient to consider $q_0 > 0$. In general, the polarization tensor in matter is a function of \vec{q} as well as of q_0 .

The angular integrals in Eq. (10) are readily performed. We find

$$\Re \Pi_1^0 = \frac{M_N^* g_\sigma g_\omega}{2\pi^2 q_z} \int k dk \frac{2E^*(k) + q^0}{E^*(k)} \ln \frac{q^2 + 2E^*(k)q^0 - 2kq_z}{q^2 + 2E^*(k)q^0 + 2kq_z} n_T(k), \quad (12)$$

$$\Im \Pi_1^0 = 0. \quad (13)$$

for $q^2 > 0$ and $q^0 > 0$.

For Π_2^0 , there are two cases. For $q_0 > 0$ and $0 < q^2 < 4M_N^{*2}$, we have

$$\Re \Pi_2^0 = \frac{M_N^* g_\sigma g_\omega}{2\pi^2 q_z} \int k dk \frac{2E^*(k) - q^0}{E^*(k)} \ln \frac{q^2 - 2E^*(k)q^0 - 2kq_z}{q^2 - 2E^*(k)q^0 + 2kq_z} n_T(k), \quad (14)$$

$$\Im \Pi_2^0 = 0. \quad (15)$$

For $q^2 > 4M_N^{*2}$, the real part reads

$$\Re \Pi_2^0 = \frac{M_N^* g_\sigma g_\omega}{2\pi^2 q_z} \int k dk \frac{2E^*(k) - q^0}{E^*(k)} \ln \left| \frac{q^2 - 2E^*(k)q^0 - 2kq_z}{q^2 - 2E^*(k)q^0 + 2kq_z} \right| n_T(k) \quad (16)$$

and the imaginary part is given by

$$\begin{aligned} \Im \Pi_2^0 = \frac{M_N^* g_\sigma g_\omega}{2\pi q_z} \int k dk \frac{2E^*(k) - q^0}{E^*(k)} \Theta \left[\left(\frac{q_z}{2} + \frac{q^0}{2} \sqrt{1 - \frac{4M_N^{*2}}{q^2}} \right) - k \right] \\ \Theta \left[k - \left(\frac{q_z}{2} - \frac{q^0}{2} \sqrt{1 - \frac{4M_N^{*2}}{q^2}} \right) \right] n_T(k) \end{aligned} \quad (17)$$

for $q^2 < 2q^0 M_N^*$ and by

$$\begin{aligned} \Im \Pi_2^0 = \frac{M_N^* g_\sigma g_\omega}{2\pi q_z} \int k dk \frac{2E^*(k) - q^0}{E^*(k)} \Theta \left[\left(\frac{q_z}{2} + \frac{q^0}{2} \sqrt{1 - \frac{4M_N^{*2}}{q^2}} \right) - k \right] \\ \Theta \left[k + \left(\frac{q_z}{2} - \frac{q^0}{2} \sqrt{1 - \frac{4M_N^{*2}}{q^2}} \right) \right] n_T(k) \end{aligned} \quad (18)$$

for $q^2 > 2q^0 M_N^*$.

The $\omega\sigma$ mixing matrix elements depend on the σNN and ωNN coupling constants, g_σ and g_ω , and on the nucleon effective mass, $M_N^*(\rho)$.

We choose $g_\sigma=12.78$ from Ref. [11]. There is some uncertainty in this quantity linked to the nature of the σ field. The Walecka Model [12] and the One-Boson-Exchange potentials [13] favor somewhat smaller values, on the order of $g_\sigma=10$.

For the ωNN coupling constant, we adopt $g_\omega=9$ as required by universality [14]. We expect this value to be the most adequate one for describing the coupling of physical ω -mesons to nucleons. In the Walecka Model, the preferred value is $g_\omega=11.7$ [12] while an even larger coupling constant $g_\omega \simeq 17$ is used in One-Boson-Exchange potentials [13]. It is likely that various

other contributions to the repulsive part of the nucleon-nucleon interaction are subsumed in the effective ω degree of freedom in these approaches.

To calculate the diagrams displayed in Fig. 2, we shall evaluate the polarization at $q^2 = m_\omega^2$. We note that, for $q^2 = m_\omega^2$, a form factor of the form $[(\Lambda^2 - m_\omega^2)/(\Lambda^2 - q^2)]^n$ at the ωNN vertex is strictly equal to unity. Similarly, a form factor of the same form at the σNN vertex, but with m_ω replaced by m_σ , is very close to unity for the same value of q^2 and for $m_\sigma=0.84$ GeV (see below). Consequently, such form factors can be neglected in our calculation.

The density dependence of the nucleon effective mass is determined within the nonlinear field theoretical approach of Ref. [15]. The Lagrangian of this model is obtained by adding nonlinear terms of the form,

$$\mathcal{L}^{NL} = -\frac{aM_N}{3}g_\sigma^3\sigma^3 - \frac{b}{4}g_\sigma^4\sigma^4, \quad (19)$$

to the Walecka scalar-vector model [12]. The parameters of the Lagrangian are fitted to give a reasonable description of the properties of nuclear matter. We impose as constraints the saturation density ($\rho_0 = 0.17 \text{ fm}^{-3}$), the binding energy per nucleon ($E/A=-16$ MeV) and the compression modulus ($K=300$ MeV). We note that this model allows for values of K much closer to the empirical value than the very large incompressibility ($K\simeq 550$ MeV) obtained in the original Walecka model [12]. Furthermore, we fix the nucleon effective mass at saturation density to be $M_N^*(\rho_0) = 0.7 M_N$, a value appropriate for particle-hole excitations involving momenta far above the Fermi surface [16]. However, since our results are very sensitive to the value of the nucleon effective mass, we also give some results obtained with $M_N^*(\rho_0) = 0.8 M_N$. The four parameters of the model are $C_\sigma = g_\sigma^2(M_N/m_\sigma)^2$, $C_\omega = g_\omega^2(M_N/m_\omega)^2$, $A = aM_Ng_\sigma^3$ and $B = bg_\sigma^4$. Their numerical values are $C_\sigma = 243.22$, $C_\omega = 145.77$, $A = 0.321 \cdot 10^{-2}$ and $B = -0.129 \cdot 10^{-2}$ for $M_N^*(\rho_0) = 0.7 M_N$ and $C_\sigma = 173.35$, $C_\omega = 85.82$, $A = 0.256 \cdot 10^{-2}$ and $B = 0.309 \cdot 10^{-1}$ for $M_N^*(\rho_0) = 0.8 M_N$.

3. $\pi\pi$ scattering phase shifts in the s-wave

We present in this section a model for $\pi\pi$ scattering in the s-wave and fix the $\sigma\pi\pi$ vertex (coupling constant and form factor in the time-like region) as well as the σ -meson mass, needed to calculate the processes illustrated in Fig. 2.

We assume that s-wave $\pi\pi$ scattering is dominated by the σ -meson in the s-channel and we compute the σ self-energy to the one-loop order, including both pion and kaon loops, as shown in Fig. 3. We remark that this approach is very different from meson-exchange models in which a potential for $\pi\pi$ scattering is generated by summing the lowest-lying s-, t- and u-channel exchange diagrams [17].

In resonant scattering, the phase shift is directly related to the resonance propagator. In our model of s-wave $\pi\pi$ scattering, the phase shift δ_0 below the $K\bar{K}$ threshold can be expressed

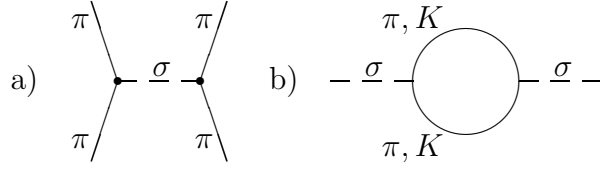


Fig. 3. $\pi\pi$ s-wave scattering (a) and σ self-energy (b).

as a function of the real and imaginary parts of the σ -meson propagator G_σ ,

$$\tan(\delta_0(q)) = \frac{\Im m G_\sigma(q)}{\Re G_\sigma(q)} = -\frac{\Im m G_\sigma^{-1}(q)}{\Re G_\sigma^{-1}(q)}, \quad (20)$$

where G_σ is defined by

$$G_\sigma(q) = \frac{1}{q^2 - m_\sigma^0 - \Sigma(q)}. \quad (21)$$

In Eq. (21), m_σ^0 is the bare σ -meson mass and $\Sigma(q)$ the self-energy associated with the π and K loops of Fig. 3b.

In order to calculate $\Sigma(q)$, we assume the following forms of the interaction Lagrangians

$$\mathcal{L}_{\sigma\pi\pi} = \frac{1}{2} g_{\sigma\pi\pi} m_\pi \bar{\pi} \pi \sigma \quad (22)$$

and

$$\mathcal{L}_{\sigma KK} = g_{\sigma KK} m_K (\bar{K}^0 K^0 \sigma + K^+ K^- \sigma). \quad (23)$$

We use extended $\sigma\pi\pi$ and σKK vertices characterized by the same functional form and cutoff,

$$F(q) = \frac{\Lambda^2}{\Lambda^2 - q^2}. \quad (24)$$

The form factor effectively accounts for higher order processes, not included in the lowest order approximation.

The self-energy $\Sigma(q)$ is given by

$$\begin{aligned} -i\Sigma(q) &= \frac{3}{2} g_{\sigma\pi\pi}^2 m_\pi^2 F^2(q^2) \int \frac{d^4 k_1}{(2\pi)^4} \frac{1}{k_1^2 - m_\pi^2 + i\epsilon} \frac{1}{(k_1 - q)^2 - m_\pi^2 + i\epsilon} \\ &\quad + 2 g_{\sigma KK}^2 m_K^2 F^2(q^2) \int \frac{d^4 k_2}{(2\pi)^4} \frac{1}{k_2^2 - m_K^2 + i\epsilon} \frac{1}{(k_2 - q)^2 - m_K^2 + i\epsilon}, \end{aligned} \quad (25)$$

where the coefficient 3/2 for the pion loop comes from the the 3 isospin states and the permutation symmetry factor and the coefficient 2 for the kaon loop accounts for the neutral and charged kaon contributions. We are interested in fitting the s-wave $\pi\pi$ phase shifts for values of \sqrt{s} of the order of the ω -meson mass, i.e. typically between $\sqrt{s} = 2m_\pi$ and $\sqrt{s} = 2m_K$. In this range, $4m_\pi^2 < q^2 < 4m_K^2$, the contribution of the pion loop to $\Sigma(q)$ has both real and imaginary parts while the contribution of the kaon loop is real.

The pion and kaon loops are logarithmically divergent. We regularize the corresponding integrals using the Pauli-Villars method [18]. We couple for each loop the σ -meson to an additional pseudoscalar field with a very large mass and multiply the regularizing integrals by constants chosen so as to remove the divergences. This procedure is discussed in detail for the calculation of the vacuum polarization in quantum electrodynamics in Ref. 19.

For $4m_\pi^2 < q^2 < 4m_K^2$, we find

$$\begin{aligned} \Re \Sigma(q) = & -\frac{3}{16\pi^2} g_{\sigma\pi\pi}^2 m_\pi^2 F^2(q^2) \left\{ \ln \frac{m_\Lambda}{m_\pi} + \frac{1}{2} \left(\frac{q^2 - 4m_\pi^2}{q^2} \right)^{1/2} \ln \left[\frac{q - (q^2 - 4m_\pi^2)^{1/2}}{q + (q^2 - 4m_\pi^2)^{1/2}} \right] \right. \\ & \left. - \frac{1}{2} \left(\frac{4m_\Lambda^2 - q^2}{q^2} \right)^{1/2} \left[2 \arctan \left(\frac{4m_\Lambda^2 - q^2}{q^2} \right)^{1/2} - \pi \right] \right\} \\ & - \frac{1}{4\pi^2} g_{\sigma KK}^2 m_K^2 F^2(q^2) \left\{ \ln \frac{m_{\Lambda'}}{m_K} \right. \\ & \left. + \frac{1}{2} \left(\frac{4m_K^2 - q^2}{q^2} \right)^{1/2} \left[2 \arctan \left(\frac{4m_K^2 - q^2}{q^2} \right)^{1/2} - \pi \right] \right. \\ & \left. - \frac{1}{2} \left(\frac{4m_{\Lambda'}^2 - q^2}{q^2} \right)^{1/2} \left[2 \arctan \left(\frac{4m_{\Lambda'}^2 - q^2}{q^2} \right)^{1/2} - \pi \right] \right\} \end{aligned} \quad (26)$$

and

$$\Im \Sigma(q) = -\frac{3}{32\pi} g_{\sigma\pi\pi}^2 m_\pi^2 F^2(q^2) \left(\frac{q^2 - 4m_\pi^2}{q^2} \right)^{1/2}, \quad (27)$$

where m_Λ and $m_{\Lambda'}$ are the Pauli-Villars masses and $q = \sqrt{q^2}$. The value of the physical mass of the σ -meson in our model is fixed by the condition

$$\Re G_\sigma^{-1}(q^2 = m_\sigma^2) = 0. \quad (28)$$

This relation provides the functional dependence of m_σ^{02} on m_σ^2 . Inserting this value of m_σ^{02} in the expression for $G_\sigma(q)$, we obtain

$$\Re G_\sigma^{-1}(q^2) = q^2 - m_\sigma^2 - (\Sigma(q^2) - \Sigma(m_\sigma^2)). \quad (29)$$

For m_Λ and $m_{\Lambda'}$ approaching infinity, the terms involving the Pauli-Villars masses vanish and the physical contribution to $\Re G_\sigma^{-1}(q^2)$ is given by the remaining terms,

$$\begin{aligned}
\Re G_\sigma^{-1}(q^2) = & q^2 - m_\sigma^2 \\
& - \frac{3}{16\pi^2} g_{\sigma\pi\pi}^2 m_\pi^2 \left\{ F^2(m_\sigma^2) \left(\frac{m_\sigma^2 - 4m_\pi^2}{4m_\sigma^2} \right)^{1/2} \ln \left[\frac{m_\sigma - (m_\sigma^2 - 4m_\pi^2)^{1/2}}{m_\sigma + (m_\sigma^2 - 4m_\pi^2)^{1/2}} \right] \right. \\
& \quad \left. - F^2(q^2) \left(\frac{q^2 - 4m_\pi^2}{4q^2} \right)^{1/2} \ln \left[\frac{q - (q^2 - 4m_\pi^2)^{1/2}}{q + (q^2 - 4m_\pi^2)^{1/2}} \right] \right\} \\
& - \frac{1}{4\pi^2} g_{\sigma KK}^2 m_K^2 \left\{ F^2(m_\sigma^2) \left(\frac{4m_K^2 - m_\sigma^2}{4m_\sigma^2} \right)^{1/2} \left[2 \arctan \left(\frac{4m_K^2 - m_\sigma^2}{m_\sigma^2} \right)^{1/2} - \pi \right] \right. \\
& \quad \left. - F^2(q^2) \left(\frac{4m_K^2 - q^2}{4q^2} \right)^{1/2} \left[2 \arctan \left(\frac{4m_K^2 - q^2}{q^2} \right)^{1/2} - \pi \right] \right\} \quad (30)
\end{aligned}$$

and

$$\Im G_\sigma^{-1}(q^2) = \frac{3}{32\pi} g_{\sigma\pi\pi}^2 m_\pi^2 F^2(q^2) \left(\frac{q^2 - 4m_\pi^2}{q^2} \right)^{1/2}. \quad (31)$$

Using Eq. (20), we can fit the s-wave $\pi\pi$ phase shift δ_0 . The result, displayed in Fig. 4, is obtained with $m_\sigma=0.84$ GeV, $g_{\sigma\pi\pi}=12.8$, $g_{\sigma KK}=8.68$ and $\Lambda=1.4$ GeV. Considering the complexity of the σ degree of freedom and the simplicity of the model, this fit is remarkably good. It is particularly precise in the region of interest for our problem, i.e. around $\sqrt{s} \simeq m_\omega$.

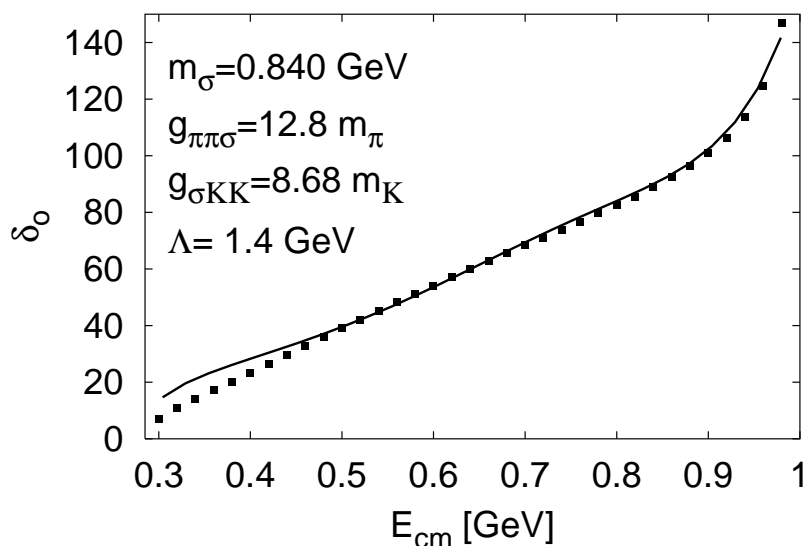


Fig. 4. Fit to the $\pi\pi$ s-wave scattering phase shift.

4. Numerical results

4.1. In-medium broadening of ω -mesons of finite momenta

In this subsection, we calculate the process illustrated in Fig. 2a. We consider an ω -meson on its mass-shell ($q^2 = m_\omega^2, q_z \neq 0$) which converts into a σ -meson through a particle-hole excitation and decays into two pions of momenta k_1 and k_2 respectively.

In the nuclear matter rest frame, the partial decay width for this process is given by [19]

$$\Gamma_{\omega \rightarrow \pi\pi} = \frac{1}{24\pi^2 q^0} \frac{3}{2} \int \frac{d^3 k_1}{2k_1^0} \frac{d^3 k_2}{2k_2^0} \sum_{spins} |M|^2 \delta^4(q - k_1 - k_2), \quad (32)$$

where M is the invariant transition matrix element and the factor $3/2$ accounts for the sum over isospin and the symmetry of the final state.

Using the interaction Lagrangian (22) and the results of Section 2, a straightforward calculation yields

$$\Gamma_{\omega \rightarrow \pi\pi} = \frac{(g_{\sigma\pi\pi} m_\pi)^2}{4\pi} F^2(q^2 = m_\omega^2) \frac{k_\pi}{4q_z^2} \frac{m_\omega}{q^0} |G_\sigma(q^2 = m_\omega^2)|^2 \Pi^{02}(q^2 = m_\omega^2, q_z), \quad (33)$$

where the form factor F is defined by Eq. (24), $k_\pi = \sqrt{m_\omega^2/4 - m_\pi^2}$ is the pion 3-momentum in the ω rest frame, G_σ and Π^0 are the σ propagator [Eqs. (30) and (31)] and the $\omega\sigma$ polarization [Eqs. 12-18] respectively.

In Figs. 5-7, we show $\Gamma_{\omega \rightarrow \pi\pi}$ as a function of density, ω -meson 3-momentum and temperature. In each figure, we indicate also the free ω width which should be added to the matter contribution (33).

We discuss first the ω broadening due to the $\omega\sigma$ polarization in nuclear matter at zero temperature (Fig. 5). The most striking result is that $\Gamma_{\omega \rightarrow \pi\pi}$ is very large. At $\rho = \rho_0$, $\Gamma_{\omega \rightarrow \pi\pi}$ is 27 MeV for $q_z = 0.5$ GeV/c, i.e. in the momentum range where the broadening is most pronounced. The reason for this is twofold. On the one hand, as already noted in Ref. [2], the $\omega\sigma$ polarization is large. On the other hand, the σ propagator taken at $q^2 = m_\omega^2$ enhances the effect. Its real part is indeed very small since our value for m_σ is close to m_ω [$m_\omega^2 - m_\sigma^2 = -0.094$ GeV²]. Furthermore, $\Gamma_{\omega \rightarrow \pi\pi}$ is also very sensitive to the nucleon effective mass. We illustrate this effect in Fig. 5 by showing the values of $\Gamma_{\omega \rightarrow \pi\pi}$ obtained for $M_N^*(\rho_0) = 0.8 M_N$. With this choice for M_N^* , $\Gamma_{\omega \rightarrow \pi\pi}$ is reduced by about 8 MeV at $\rho = \rho_0$. We note that, in the range of densities considered in Fig. 5, the $\omega\sigma$ polarization is real because $q^2 = m_\omega^2$ is always $< 4M_N^{*2}$. Hence, the in-medium width is due solely to the two-pion final state. As expected, $\Gamma_{\omega \rightarrow \pi\pi}$ exhibits a strong dependence on the baryon density.

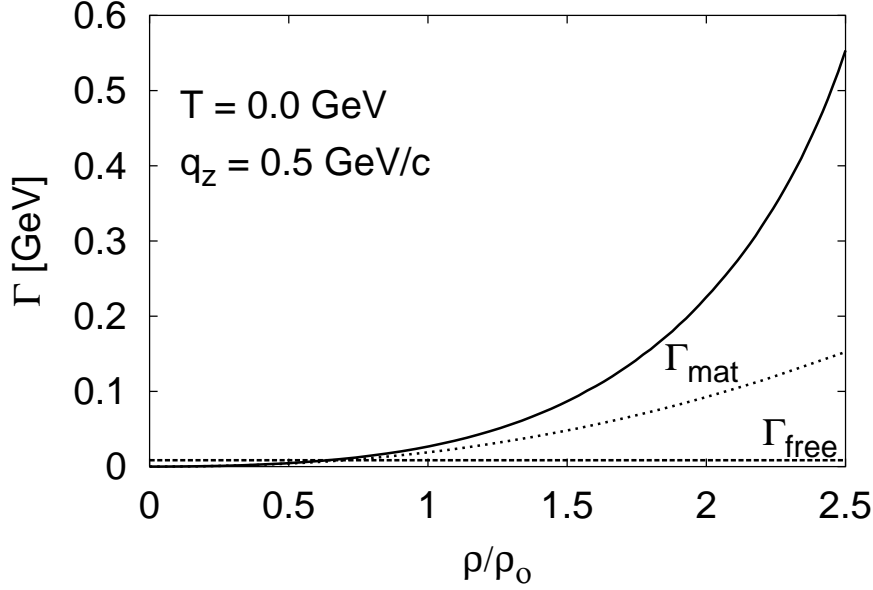


Fig. 5. Density dependence of $\Gamma_{\omega \rightarrow \pi\pi}$ (denoted Γ_{mat}) at $T=0$ and for an ω 3-momentum $q_z = 0.5$ GeV/c. The full curve is the result obtained with $M_N^*(\rho_0) = 0.7 M_N$; the dotted line shows the effect of using $M_N^*(\rho_0) = 0.8 M_N$ instead. Γ_{free} is the ω width in free space (dashed line).

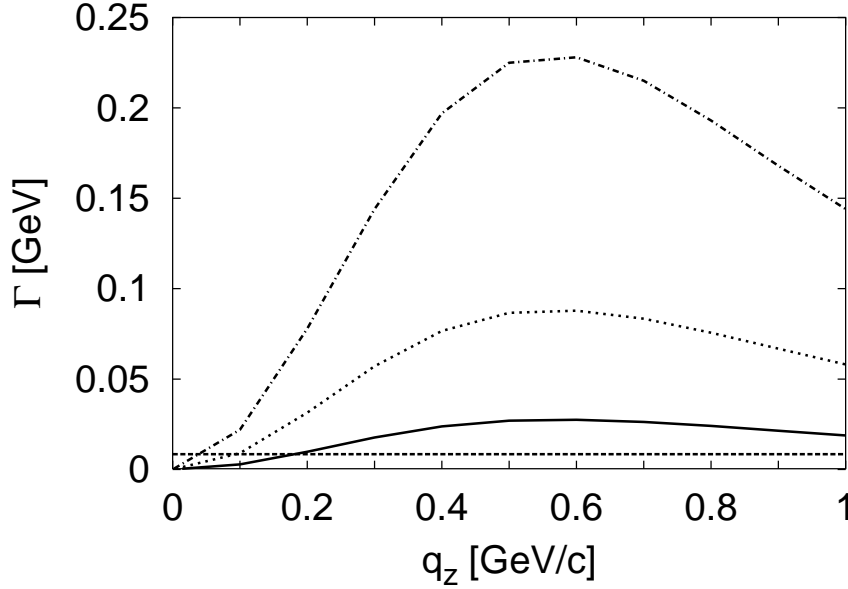


Fig. 6. Momentum dependence of $\Gamma_{\omega \rightarrow \pi\pi}$ at $T=0$ and for 3 values of the matter density $\rho/\rho_0 = 1$ (full line), 1.5 (dotted line) and 2 (dot-dashed line). The free width is indicated by a dashed line.

The 3-momentum dependence of $\Gamma_{\omega \rightarrow \pi\pi}$, displayed in Fig. 6 at $T=0$ for $\rho/\rho_0=1, 1.5$ and 2, illustrates the kinematic conditions under which the broadening of the ω -meson due to the $\omega\sigma$ polarization is the largest. At $q_z = 0$, where the $\omega\sigma$ mixing is not allowed, $\Gamma_{\omega \rightarrow \pi\pi}$ vanishes. As a consequence of the kinematic factors in Eq. (33), the initial growth of $\Gamma_{\omega \rightarrow \pi\pi}$ with q_z saturates, and is reversed for $q_z > 0.6$ GeV/c.

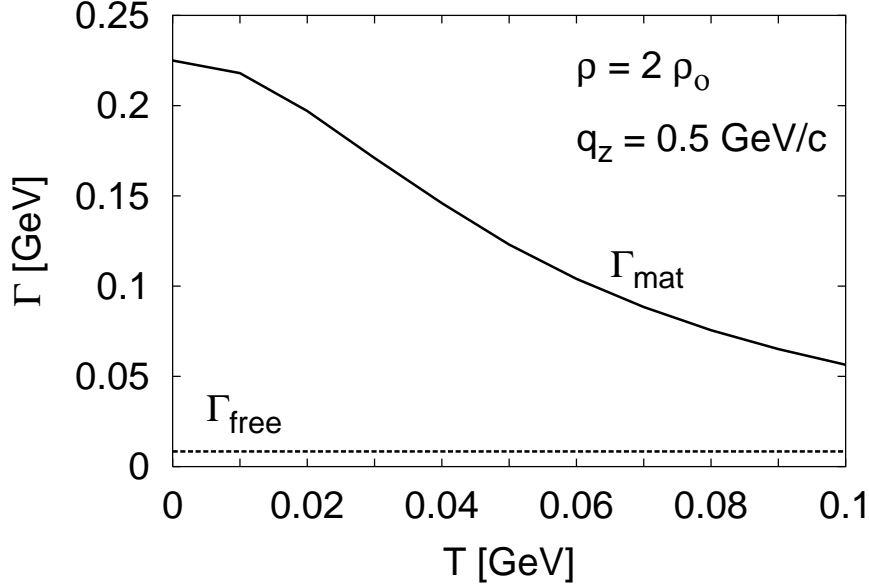


Fig. 7. Temperature dependence of $\Gamma_{\omega \rightarrow \pi\pi}$ (denoted Γ_{mat}) at $q_z = 0.5$ GeV/c and for $\rho/\rho_0 = 2$ (full line). Γ_{free} is the ω width in free space (dashed line).

In Fig. 7, we show the temperature dependence of $\Gamma_{\omega \rightarrow \pi\pi}$ for $\rho/\rho_0=2$ and $q_z = 0.5$ GeV/c. The in-medium ω width due to $\omega\sigma$ mixing decreases with increasing temperature, as a consequence of the change in occupation probability of the Fermi states. For the temperatures expected to prevail in relativistic heavy ions collisions ($E/A \simeq 1-2$ GeV), $\Gamma_{\omega \rightarrow \pi\pi}$ is decreased by at least a factor of two compared to the $T=0$ value at the same density. However, at these temperatures, collisional broadening is, as discussed above, expected to strongly enhance the in-medium width of the ω meson.

4.2. S-wave $\pi^+\pi^-$ annihilation into e^+e^- pairs

We discuss now the process illustrated in Fig. 2b and study its importance in the production of e^+e^- pairs in relativistic heavy ion collisions.

We calculate the s-wave annihilation of two pions ($\pi^+\pi^-$ or $\pi^0\pi^0$) of momenta p_1 and p_2 such that $(p_1 + p_2)^2 = m_\omega^2$. They annihilate in the σ channel which, through particle-hole excitations, mixes with the ω -meson. The ω decays into an electron and a positron of momenta k_1 and k_2 . The diagram of Fig. 2b is evaluated in the rest frame of the nuclear medium (which we identify with the interaction region in central heavy ion collisions). For each initial state ($\pi^+\pi^-$, $\pi^-\pi^+$ and $\pi^0\pi^0$), the annihilation cross section is given by

$$\sigma_{\pi\pi \rightarrow e^+e^-} = \frac{1}{8\pi^2 m_\omega} \frac{m_e^2}{\sqrt{m_\omega^2 - 4m_\pi^2}} \int \frac{d^3k_1}{k_1^0} \frac{d^3k_2}{k_2^0} \sum_{spins} |M|^2 \delta^4(p_1 + p_2 - k_1 - k_2). \quad (34)$$

The calculation of this cross section involves the same quantities as the partial decay width of Eq. (33). We use the additional assumption of vector meson dominance for the electro-

magnetic current [20]. The conversion of an ω -meson into a massive photon is characterized by the coupling constant

$$f_\omega = \frac{em_\omega^2}{2g_\omega}. \quad (35)$$

Neglecting the electron mass compared to the electron momentum, we obtain for the annihilation cross section

$$\begin{aligned} \sigma_{\pi\pi \rightarrow e^+e^-} = & \frac{\pi}{3q_z^2} \frac{m_\omega^3}{\sqrt{q^2 - 4m_\pi^2}} \left(\frac{\alpha}{g_\omega} \right)^2 (g_{\sigma\pi\pi} m_\pi)^2 \frac{1}{(q^2 - m_\omega^2)^2 + m_\omega^2 \Gamma_\omega^{tot2}} F^2(q^2) \\ & \times |G_\sigma(q^2)|^2 \Pi^{02}(q^2, q_z). \end{aligned} \quad (36)$$

The width Γ_ω^{tot} entering in Eq. (36) is the sum of $\Gamma_{\omega \rightarrow \pi\pi}$ given by Eq. (33) and of the ω width in free space, Γ_ω^{free} . This expression includes therefore the in-medium broadening of the ω -meson discussed in 4.1.

In calculations [21-23] of the production of e^+e^- pairs in relativistic heavy ion collisions, without medium effects, the invariant mass spectrum in the range $0.6 < m_{e^+e^-} < 0.9$ GeV is dominated by p-wave $\pi^+\pi^-$ annihilation in the ρ -meson channel and by the decay of direct ω mesons (those produced in baryon-baryon collisions) The direct ρ -mesons play a minor role.

Using transport equations based on the Boltzmann-Uehling-Uhlenbeck approximation [21-23], we have calculated differential cross sections for the production e^+e^- pairs in the invariant mass interval $0.6 < m_{e^+e^-} < 0.9$ GeV in central $^{58}\text{Ni} + ^{58}\text{Ni}$ collisions at 2 GeV per nucleon. For the evaluation of the $\omega\sigma$ mixing, we assume a temperature of 80 MeV in the interaction region. We consider the three processes mentioned above ($\pi^+\pi^- \rightarrow \rho \rightarrow e^+e^-$, $\rho \rightarrow e^+e^-$ and $\omega \rightarrow e^+e^-$) as well as the process studied in this paper, $\pi\pi \rightarrow \omega \rightarrow e^+e^-$.

In the total invariant mass spectra for these processes (Fig. 8a), the s-wave $\pi\pi$ annihilation does not play an important role. Thus, it is unlikely that it gives rise to an observable effect.

The momentum-dependent broadening of the ω -meson reduces the ω -peak below the p-wave $\pi^+\pi^-$ annihilation in the total invariant mass spectrum. With transverse momentum cuts, $q_t < 0.1$ GeV (Fig. 8b) and $q_t > 0.2$ GeV (Fig. 8c), it may be possible to explore those effects in experiments. However, before further conclusions can be drawn, other momentum-dependent corrections to the propagation of ω -mesons in matter must be investigated.

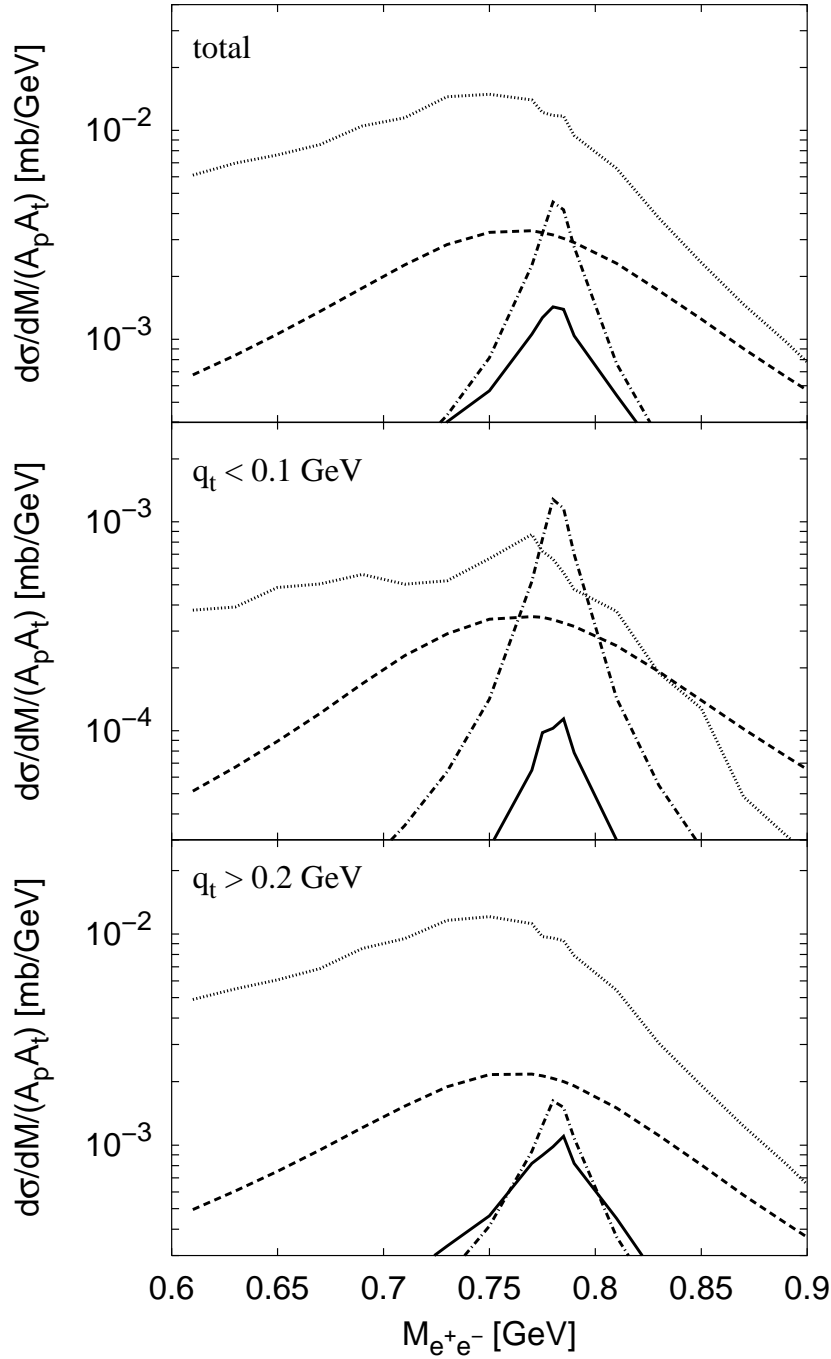


Fig. 8. Dilepton invariant mass spectra for $^{58}\text{Ni}+^{58}\text{Ni}$ central collisions at 2 GeV per nucleon. The four curves in each figure show the e^+e^- spectra induced by direct or intermediate ρ and ω decays. The dotted line corresponds to the dominant $\pi^+\pi^- \rightarrow \rho \rightarrow e^+e^-$ process. The dashed line shows the contribution of the e^+e^- pairs due to the direct ρ mesons, while the dot-dashed one shows that of the direct ω mesons. Finally, the solid line represents the effect of the process discussed in this paper, $\pi\pi \rightarrow \omega \rightarrow e^+e^-$. In (a) the spectra obtained with all events are shown, while in (b) and (c) the transverse momentum cuts $q_t < 0.1$ GeV and $q_t > 0.2$ GeV were applied.

5. Conclusion

We have investigated in this paper two consequences of the large value of the nondiagonal $\omega\sigma$ polarization in matter at zero and finite temperature.

Our most important result is a substantial broadening of ω -mesons moving with respect to a nuclear medium. The additional width, arising from the conversion of ω -mesons into σ -mesons through particle-hole excitations and the subsequent decay of the σ into two pions, can be much larger than the free width. At $T=0$, this in-medium width increases with density and with the 3-momentum of the ω -meson for $q \lesssim 0.5$ GeV/c. As a function of temperature, the effect decreases with increasing temperature. Our results are therefore most relevant for the studies of the propagation of ω -mesons in nuclei. In particular, the in-medium broadening of the ω meson should have observable consequences in experiments where ω -mesons are produced in heavy nuclear targets and observed in the e^+e^- decay channel [4-5]. As already emphasized, collisional broadening from the $\omega N \rightarrow \pi N$ and $\omega N \rightarrow \rho N$ reactions is expected to lead to a substantial further increase of the ω width in matter. All these processes should be included consistently in a calculation of the ω propagator at finite baryon density.

Our study of the inverse process, the s-wave $\pi^+\pi^-$ annihilation producing an ω -meson which decays into an e^+e^- pair, has shown that its contribution to dilepton spectra is much smaller than the that of p-wave $\pi^+\pi^-$ annihilation in the ρ -channel. Consequently, we do not expect observable effects of this process in the dilepton mass spectrum. However, the momentum dependent broadening of the ω meson may lead to a detectable effect also in heavy-ion collisions, once momentum cuts are applied.

Acknowledgements

Two of us (M. S. and Gy. W.) acknowledge gratefully the hospitality of GSI where much of this work was done. Gy. W. was supported in part by the Hungarian Research Foundation OTKA (grants T022931 and T016594).

References

- [1] G.E. Brown and W. Weise, Phys. Rep. 22 (1975) 279.
- [2] L.S. Celenza, A. Pantziris and C.M. Shakin, Phys. Rev. C45 (1992) 205.
- [3] G.E. Brown and M. Rho, Phys. Rev. Lett. 66 (1991) 2720.
- [4] CEBAF Proposal PR 89-001, Nuclear mass dependence of vector mesons using the photoproduction of lepton pairs, Spokesmen: D. Heddle and B.M. Freedom; CEBAF Proposal PR 94-002, Photoproduction of vector mesons off nuclei, Spokesmen: P.-Y. Bertin, M. Kossov and B.M. Freedom.
- [5] HADES Proposal (GSI Internal Report) and private communication.
- [6] Review of Particle Properties, Phys. Rev. D54 (1996) 1.
- [7] F. Klingl, N. Kaiser and W. Weise, to be published, hep-ph/9704398.
- [8] H. Karami et al, Nucl. Phys. B154 (1979) 503; J. S. Danbury et al, Phys. Rev. D2 (1970) 2564.
- [9] P. A. Henning and B. L. Friman, Nucl. Phys. A490 (1988) 689.
- [10] K. Lim and C. J. Horowitz, Nucl. Phys. A501 (1989) 729.
- [11] J.W. Durso, A.D. Jackson and B.J. VerWest, Nucl. Phys. A345 (1980) 471.
- [12] B.D. Serot and J. D. Walecka, Adv. Nucl. Phys. 16 (1986) 1.
- [13] R. Machleidt, Adv. Nucl. Phys. 19 (1989) 189.
- [14] U.G. Meissner, Phys. Rep. 161 (1988) 213.
- [15] J. Boguta and A. R. Bodmer, Nucl. Phys. A292 (1977) 413.
- [16] C. Mahaux et al, Phys. Rep. 120 (1985) 1; G.E. Brown, J.H. Gunn and P. Gould, Nucl. Phys. 46 (1963) 598.
- [17] G. Janssen et al, Phys. Rev. D52 (1995) 2690.
- [18] W. Pauli and F. Villars, Rev. Mod. Phys. 21 (1949) 434.
- [19] C. Itzykson and J.-B. Zuber, Quantum Field Theory, McGraw-Hill, 1980.
- [20] N.M. Kroll, T.D. Lee and B. Zumino, Phys. Rev. 157 (1967) 1376.
- [21] Gy. Wolf et al, Nucl. Phys. A517 (1990) 615.
- [22] Gy. Wolf, W. Cassing and U. Mosel, Nucl. Phys. A 552 (1993) 549.
- [23] Gy. Wolf, Acta Phys. Pol. B26 (1995) 583.